

Magnetic resonance effect in x-ray resonant Raman scattering

T. Iwazumi, K. Kobayashi,* and S. Kishimoto

Photon Factory, Institute of Materials Structure Science, 1-1 Oho, Tsukuba 305, Japan

T. Nakamura and S. Nanao

Institute of Industrial Science, University of Tokyo, 7-22-1 Roppongi, Minato 106, Japan

D. Ohsawa and R. Katano

Institute for Chemical Research, Kyoto University, Uji 611, Japan

Y. Isozumi

Radioisotope Research Center, Kyoto University, Kyoto 606-01, Japan

(Received 9 June 1997)

The magnetic-circular-dichroism spectra of the x-ray resonant Raman scattering associated with the Gd $L\alpha_1$, $L\alpha_2$, and $L\beta_{2,15}$ fluorescence lines of the ferrimagnetic Gd-Co compound are presented. The incident x-ray energy dependence of these spectra clearly shows not only normal resonance effects, but also magnetic resonance effects between the excited $2p_{3/2}$ electron and the $5d$ valence state, i.e., an enhancement of the magnetic effects and the appearance of a structure that corresponds to the magnetic effect of the total fluorescence yield. [S0163-1829(97)50346-8]

Intense, energy-tunable, highly polarized x rays obtained by synchrotron radiation have created new possibilities in studying the electronic and magnetic structures of solids using inelastic x-ray scattering. A few years ago Ma *et al.* discovered the interference effect of x-ray resonant Raman scattering (XRRS),¹ and Krisch *et al.* provided experimental evidence that we can obtain information about the conduction states by using XRRS.² Recent theoretical work also suggests that the spectra of the low-energy off-resonance of XRRS, i.e., the Raman component, reflect the joint density of states of the conduction band and the valence one under the condition that the total momentum of the electron-hole pair left at the final state is zero.³ More recently, Krisch *et al.* reported on the magnetic circular dichroism (MCD) of the x-ray fluorescence spectroscopy (XFS) data of the Gd $L\alpha_1$ and $L\beta_{2,15}$ lines of Gd metal,⁴ and the theoretical calculation of these spectral shapes was performed using a theoretical description of spin-polarized $2p$ -photoemission and atomic-multiplet calculations of the $2p3d$ and $2p4d$ radiative decay.⁵

In this paper we present the full spectra of the MCD of the x-ray emission spectroscopy (XES), i.e., the MCD-XFS of Gd $L\alpha_1$, $L\alpha_2$, and $L\beta_{2,15}$ lines and the MCD-XRRS associated with these three fluorescence lines of the ferrimagnetic Gd-Co compound, whose incident photon energies are around the Gd L_{III} absorption edge. The incident x-ray energy dependence of the XES shows clear resonance effects between the excited $2p_{3/2}$ electron and the $5d$ valence state when the incident photon energy is at the exact absorption edge: the increase and narrowing of the spectral features, and the existence of an energy shift between the low-energy off-resonant XRRS and the high-energy off-resonant one. That of the MCD-XES shows a similarity between the MCD-XRRS corresponding to the dipolar $2p_{3/2} \rightarrow 5d$ transition and the MCD-XFS, and suggests that the spin polarization of the

$5d$ state of Gd is similar to that of the $3d$ or $4d$ states. Moreover, when the incident photon energies are at the exact absorption edge, the MCD-XRRS clearly exhibits resonance effects, i.e., the enhancement of the magnetic effects and the appearance of a new structure corresponding to the magnetic effect of the total fluorescence yield.

The experiment was performed at the elliptical multipole wiggler beamline (28B) of the Photon Factory, Institute of Materials Structure Science.⁶ This beamline is equipped with focusing optics using a double-crystal monochromator between the two bent mirrors, and provides a 2.3 mm horizontal and 0.3 mm vertical focused beam. With a Si(111) monochromator, the flux of the incident beam is estimated to be $\sim 10^{11}$ photons/s, and the degree of circular polarization of this beam is not known in the energy range around the Gd L_{III} edge, but may not be very different from $P_c = -0.41$ measured at 7.7 keV. The sample used in this experiment was an amorphous Gd-Co sputtered on a polyimide film. The composition of Gd-Co was 33 at. % Gd and 67 at. % Co, measured by the inductively coupled plasma method. The sample film was mounted at the focus point and between the pole pieces of an electromagnet so that the magnetization of the sample could be reversed periodically.

The scattered radiation was analyzed at a 55° scattering angle in the vertical plane by a cylindrically bent Ge(333) crystal for the energy range around the Gd $L\alpha$ fluorescence lines and at 54° by InSb(444) for Gd $L\beta$. The analyzed x-rays were detected by a position-sensitive proportional counter (PSPC) with the charge-division method. The resistive anode of the PSPC was a carbon fiber $7 \mu\text{m}$ in diameter, and its resistance was $4.2 \text{ k}\Omega$ per cm. The entrance window was made of a 1-mm-thick beryllium plate, and the sensitive area of the window was $10 \times 100 \text{ mm}^2$. The distance between the anode and the entrance window was 10 mm. The pressure of the flow gas (Ar+10% CH₄) was controlled to be 8

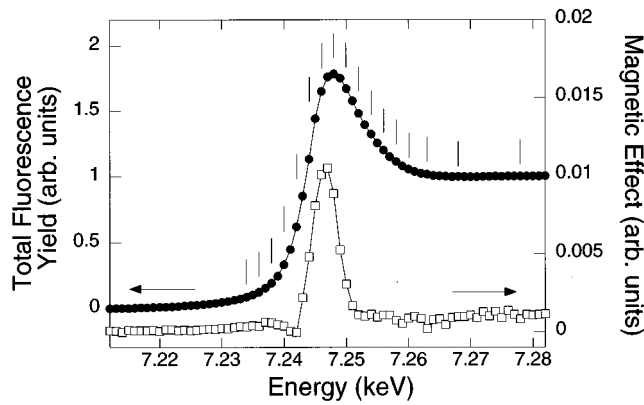


FIG. 1. Total fluorescence yield and its magnetic effect of Gd in Gd-Co around the L_{III} edge of Gd. The vertical lines correspond to the incident photon energies at which emission spectroscopy measurements were performed.

atm. An efficiency calibration along the anode direction was made using 5.9 keV Mn K x rays from a ^{55}Fe radioactive source. Both the sample and the detector were arranged on the center axis of the analyzing crystal cylinder, so that we could obtain sagittal-focused and meridional-energy dispersive x rays. The typical counting rate at the Gd $L\alpha_1$ fluorescence peak was 200 cps, and that of the full energy range around the Gd $L\alpha$ fluorescence lines was on the order of 4000 cps. The total energy resolutions of the present apparatus are 1.4 eV around the Gd $L\alpha$ fluorescence lines and 1.8 eV around Gd $L\beta$. Incident x rays have a left-circular polarization with -1 helicity. We define the positive (negative) direction of a magnetic field when the \mathbf{B} vector is directed parallel (antiparallel) to the x-ray wave vector. The magnetic effect was defined as subtracting the fluorescent x rays detected on the positive direction from that of the negative one,

and the normalized magnetic effect was defined as dividing the magnetic effect by the sum.

Figure 1 shows the total fluorescence yield spectrum and its magnetic effects around the Gd L_{III} absorption edge, measured from the same specimen used in the XES study. The total fluorescence yield was measured using the normal fluorescence ion chamber. These features are essentially identical to the XAS and MCD-XAS spectra of the Gd metal and its compounds.⁷ The vertical lines in the figure correspond to the incident photon energies at which the XES measurements were performed.

The XES spectra around the Gd $L\alpha$ fluorescence lines are shown in Fig. 2(a). The small irregularities around 6.023 keV are due to the imperfection of the efficiency calibration of the PSPC. The observed structures in these XES spectra can be divided into five groups (labeled A, B, C, D, and E in the figure); these peak positions are plotted as a function of the incident photon energy in Fig. 3. As shown in Fig. 3, the peak energies of peaks A, B, and C, whose incident photon energies were above 7250 eV, are constant. These peaks (A, B, and C) correspond to the normal fluorescence lines: $L\alpha_2$, $L\alpha_1$ satellite from multiplet splitting,⁸ and $L\alpha_1$, respectively. The peak energies of peaks A, B, and C, whose incident photon energies were below 7250 eV, and peaks D and E, increased with increasing incident energy. These peaks correspond to XRRS. Peaks A, B, and C below 7250 eV are associated with the normal fluorescence lines ($L\alpha_2$, $L\alpha_1$ satellite, and $L\alpha_1$). Peak D is the high-energy off-resonant XRRS relevant to the $L\alpha_1$ fluorescence line, which is an unusual structure in the hard x-ray region. Peak E is assigned to the multiplet of the $2p^{54}f^{n+1}$ quadrupolar excitation.² In Fig. 2(a) it is evident that the features of the XRRS peaks increase and narrow when the incident photon energies are at the exact absorption edge. These phenomena

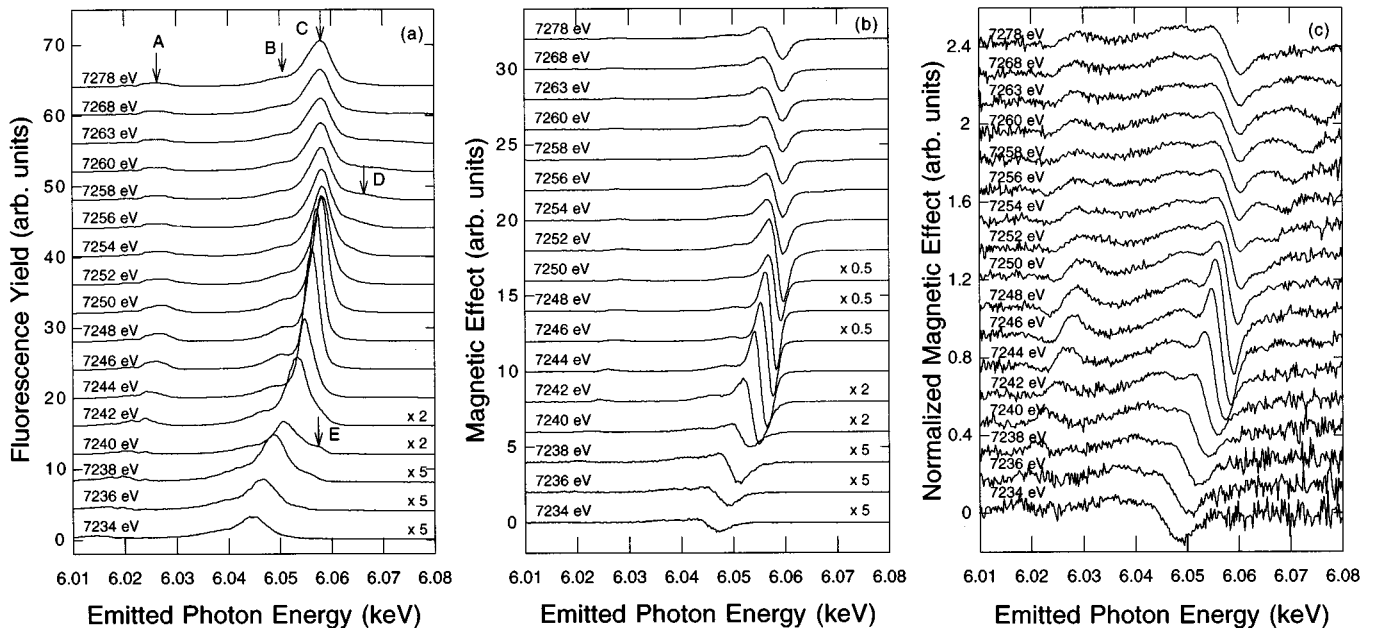


FIG. 2. (a) X-ray emission spectra around the Gd $L\alpha$ fluorescence from Gd-Co. The incident photon energy at which the spectra were taken is given in the figure. They are divided into five groups labeled by the corresponding scaling factor. (b) Magnetic effects of the x-ray emission spectra. (c) Normalized magnetic effects of the x-ray emission spectra.

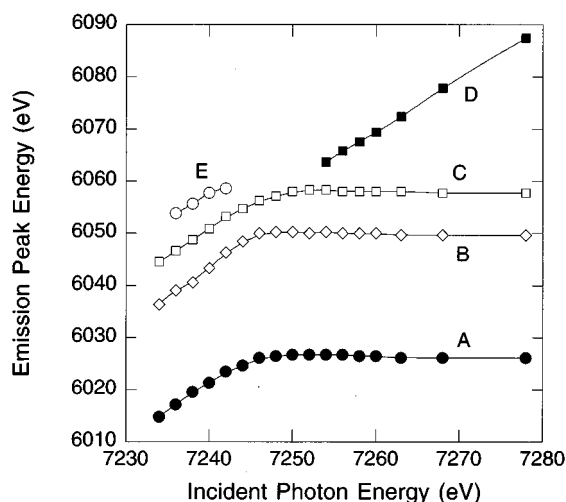


FIG. 3. Incident photon-energy dependence of the emission peak energy of the five groups (A, B, C, D, and E) indicated in Fig. 2(a).

are the resonance effects between the excited $2p_{3/2}$ electron and the $5d$ valence state of Gd.⁹ Although peaks C below 7250 eV and D are the XRRS associated with the same fluorescence line, these two linear dependences of the peak position show a discontinuity at the Gd L_{III} absorption edge, whose shift value is about 1 eV for the incident photon energy, as shown in Fig. 3. This energy shift is additional evidence of the resonance effect.¹⁰

Figure 2(b) exhibits magnetic effects of the XES spectra in Fig. 2(a). The magnetic effects of the normal fluorescence lines, whose incident photon energies were above 7254 eV, show many of the same features as those of the Gd metal,⁴ and a clearer separation between the diagonal lines and these satellites. The shapes of the magnetic effects of XRRS associated with the normal fluorescence lines, whose incident photon energies were below 7240 eV, are almost the same as those of the normal fluorescence lines above 7254 eV. This result suggests that the spin polarization of the $5d$ state of

Gd is similar to that of the $3d$ states. The magnetic effects of peak E are always negative, which is consistent with the spin-down character of the empty $4f$ states, as pointed out before.⁴ To compare the magnitude of the magnetic effects, the normalized magnetic effects of the XES spectra are shown in Fig. 2(c). From this figure it is evident that an enhancement of the normalized magnetic effects occurs in the narrow energy region of the incident x rays between 7242 and 7252 eV. The maximum value of the normalized magnetic effect increases from 40% to 90% when corrected for the geometrical factor of the incident photons and the magnetic field direction, and the incoming photon polarization. Moreover, the shape change for the easiest example the positive growth at the low-energy side of peak C was found in the same energy region of the incident x rays. This new structure corresponds to a positive magnetic effect of the total fluorescence yield, as can be seen in the bottom curve of Fig. 1. Because the energy region of incident x rays agrees almost with the exact absorption edge in which the resonance effects in the normal XRRS are found, as mentioned above, these magnetic features can be assigned to the magnetic resonance effects between the excited $2p_{3/2}$ electron and the $5d$ valence state. These magnetic resonance effects should reflect changes in spin-orbit couplings and the Slater integrals of the final-state configurations.⁵

The XES spectra, the corresponding magnetic effects, and the normalized magnetic effects around the Gd $L\beta_{2,15}$ fluorescence line are shown in Figs. 4(a), 4(b), and 4(c), respectively. There are clearly two groups, which are labeled F and G in Fig. 4(a). Peaks F and G correspond to the normal fluorescence lines, $L\beta_{2,15}$ satellite from multiplet splitting and $L\beta_{2,15}$, respectively, and the XRRS associated with these two fluorescence lines. Almost the same feature can be seen with peaks B and C in Fig. 2, except for the energy separation between the diagonal line and its satellite from multiplet splitting. From Fig. 4 we conclude that the spin polarization of the $5d$ state of Gd is similar to that of $4d$ states, and that the enhancement of the magnetic effects also occurs at the exact absorption edge. The maximum value of the normalized magnetic effect goes up to 50% with a correction.

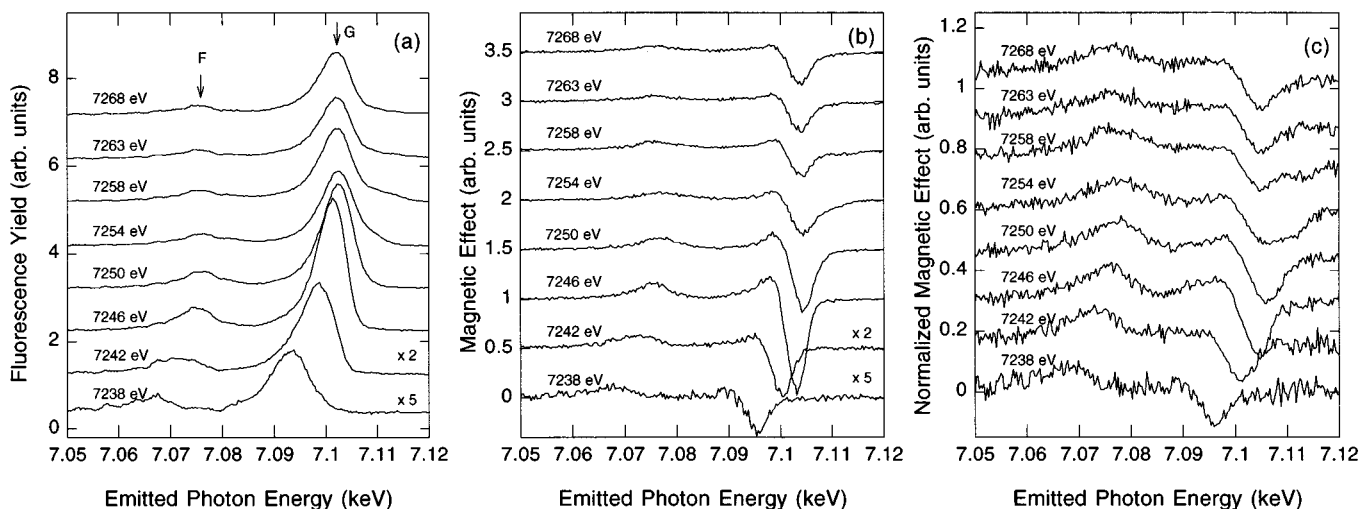


FIG. 4. (a) X-ray emission spectra around Gd $L\beta$ fluorescence from Gd-Co. The incident photon energy at which the spectra are taken is given in the figure. (b) Magnetic effects of the x-ray emission spectra. (c) Normalized magnetic effects of the x-ray emission spectra.

In summary, we have found magnetic resonance effects between the excited electron and the valence state in MCD-XRRS. The appearance of the new magnetic structure around the absorption edge, which was expected from MCD-XAS, has been confirmed. Although more than double enhancement, the magnetic effects show clear evidence of magnetic resonance, the origin of this behavior is still not well understood. Because MCD-XRRS shows extremely large magnetic signals and enhancement at the exact absorption edge, it may be possible to observe magnetic signals even from paramagnetic materials whose magnetic susceptibilities are

very small. Using the interference effects of MCD-XRRS, it is possible to obtain information on magnetic band structures.

The authors would like to thank Dr. A. Iida, Dr. K. Nasu, Dr. T. Koide, Dr. T. Minami, and Dr. K. Iwano for useful discussions on emission spectroscopy. They also acknowledge Dr. H. Hayashi and Dr. Y. Udagawa for their advice for the emission spectrometer. This work was performed with the approval of the Photon Factory Advisory Committee (Proposal No. 95G358).

*Present address: Fundamental Research Laboratories, NEC Corporation, 34 Miyukigaoka, Tsukuba 305, Japan.

¹Y. Ma, K. E. Miyano, P. L. Cowan, Y. Aglitzkiy, and B. A. Karlin, *Phys. Rev. Lett.* **74**, 478 (1995).

²M. H. Krisch, C. C. Kao, F. Sette, W. A. Caliebe, K. Hämäläinen, and J. B. Hastings, *Phys. Rev. Lett.* **74**, 4931 (1995).

³T. Minami and K. Nasu (unpublished).

⁴M. H. Krisch, F. Sette, U. Bergmann, C. Masciovecchio, R. Verbeni, J. Goulon, W. Caliebe, and C. C. Kao, *Phys. Rev. B* **54**, R12673 (1996).

⁵F. M. F. de Groot, M. Nakazawa, A. Kotani, M. H. Krisch, and F. Sette (unpublished).

⁶T. Iwazumi, A. Koyama, and Y. Sakurai, *Rev. Sci. Instrum.* **66**, 1691 (1995).

⁷For example: G. Schütz, M. Knulle, R. Wienke, W. Wilhelm, W. Wagner, P. Kienle, and R. Frahm, *Z. Phys. B* **73**, 67 (1988); K. Kobayashi, H. Maruyama, H. Yamazaki, Y. Watanabe, S. Nanao, and S. Ishio, *J. Magn. Magn. Mater.* **140–144**, 283 (1995).

⁸For example: K. Tsutsumi, *J. Phys. Soc. Jpn.* **14**, 1696 (1959); S. I. Salem and B. L. Scott, *Phys. Rev. A* **9**, 690 (1974); K. Hämäläinen, C. C. Kao, J. B. Hastings, D. P. Siddons, L. E. Berman, V. Stojanoff, and S. P. Cramer, *Phys. Rev. B* **46**, 14274 (1992).

⁹T. Åberg and J. Tulkki, in *Atomic Inner-Shell Physics*, edited by B. Crasemann (Plenum, New York, 1985).

¹⁰T. Minami and K. Nasu (private communication).